



Journal of Experimental Biology and Agricultural Sciences

<http://www.jebas.org>

ISSN No. 2320 – 8694

In-vitro antibacterial activity, Molecular docking, and MD Simulation Analysis of Phytoconstituents of *Nasturtium officinale*

 Nitisha Negi^{1,2} , Sukirti Upadhyay¹ , Bhuwan Chandra Joshi² , Prinsa³ , Supriyo Saha^{4*} 
¹School of Pharmaceutical Sciences, IFTM University, Moradabad-244102, U.P., India²Department of Pharmaceutical Sciences, Faculty of Technology, Sir J.C. Bose Technical Campus, Bhimtal, Kumaun University, Nainital-263136, Uttarakhand, India³Department of Pharmaceutical Chemistry, Siddhartha Institute of Pharmacy, Near IT-Park, Sahastradhara Road, Dehradun-248001, Uttarakhand, India⁴Department of Pharmaceutical Chemistry, Uttaranchal Institute of Pharmaceutical Sciences, Uttaranchal University, Dehradun-248007, Uttarakhand, India

Received – September 06, 2024; Revision – December 19, 2024; Accepted – December 30, 2024

Available Online – January 15, 2025

DOI: [http://dx.doi.org/10.18006/2024.12\(6\).838.849](http://dx.doi.org/10.18006/2024.12(6).838.849)

KEYWORDS

*Nasturtium officinale**Staphylococcus aureus*

Antibacterial activity

TLC fingerprint

Molecular docking

MD Simulation

ABSTRACT

Medicinal plants play a significant role in various traditional medicine systems worldwide. *Nasturtium officinale* W.T. Aiton, commonly known as ‘Halim,’ is a herbaceous perennial often used for its multiple health benefits. It serves as a depurative, diuretic, expectorant, hypoglycemic, hypolipidemic, and odontalgic agent and is utilized in the management of various ailments and disorders. This study aimed to evaluate the antimicrobial efficacy of different solvent extracts of *N. officinale* against *Staphylococcus aureus*. The antimicrobial activity was assessed through an in vitro assay using the disk diffusion method. Additionally, the minimum inhibitory concentration (MIC) was determined in comparison with standard reference compounds. Among the extracts tested, the chloroform extract of *N. officinale* (NOCE) exhibited the most potent inhibitory effect, demonstrating significant antibacterial activity. The high efficacy of the NOCE suggests that it may contain active phytoconstituents capable of targeting bacterial strains. Furthermore, molecular docking studies revealed that the phytoconstituents isorhamnetin, luteolin, and quercetin exhibited strong interactions with bacterial DNA gyrase. The molecular dynamics (MD) simulation of the best-docked compound, isorhamnetin, against bacterial DNA gyrase indicated that all parameters were within acceptable limits, and the compound effectively interacted with the receptor. These findings confirm that *N. officinale* possesses potential antibacterial activity, which may be attributed to the presence of isorhamnetin.

* Corresponding author

E-mail: supriyo9@gmail.com (Supriyo Saha)

Peer review under responsibility of Journal of Experimental Biology and Agricultural Sciences.

 Production and Hosting by Horizon Publisher India [HPI]
 (<http://www.horizonpublisherindia.in/>).
 All rights reserved.

 All the articles published by [Journal of Experimental Biology and Agricultural Sciences](#) are licensed under a [Creative Commons Attribution-NonCommercial 4.0 International License](#) Based on a work at www.jebas.org.


1 Introduction

Nasturtium officinale (*N. officinale*), also known as watercress, is a perennial herb that typically floats and creeps in water, commonly found near brooks, ditches, and ponds, especially in damp areas. This plant is native to Asia and North Africa and is rich in various vitamins, including vitamins A, C, and alpha-tocopherol (Shakerinasab et al. 2024). Additionally, *N. officinale* contains a high proportion of carotenoids, polyphenols, glucosinolates, and chlorophyll, according to previous reports. The herb is valued for both culinary and medicinal purposes. Traditionally, it has been used to treat respiratory conditions, diabetes, tuberculosis, and ailments affecting the kidneys, stomach, and liver (Negi et al. 2024a). Moreover, *N. officinale* is well-known for its anti-inflammatory, antimicrobial, antioxidant, anti-genotoxic, and cardioprotective properties (Klimek-Szczykutowicz et al. 2018). It is commonly used as a vegetable to enhance the flavor of various dishes and recipes (Mostafazadeh et al. 2022). This plant is composed of different phytochemicals, with phenolic compounds considered significant bioactive substances (Hibbert et al. 2023). The rich composition of *N. officinale* contributes to its nutritional and medicinal potential, making it a beneficial addition to a balanced diet (Klimek-Szczykutowicz et al. 2018). Various phytoconstituents exhibit different pharmacological activities, such as anti-inflammatory, anticancer, antioxidant, and antibacterial effects (Shakerinasab et al. 2024). The aerial parts of *N. officinale* are particularly notable for their medicinal significance, as they contain a higher concentration of phytoconstituents (Tabesh et al. 2022). These bioactive compounds act as a natural defense mechanism, aiding in the treatment of illnesses and protecting the human body from oxidative stress. Despite the numerous nutraceutical and ethnomedicinal uses of this plant, there have been no detailed analyses of molecular docking and molecular dynamics simulations related to its phytochemicals and pharmacological properties (Akbari Bazm et al. 2019). Consequently, the current study aims to evaluate the in vitro antibacterial properties of *N. officinale* and identify the phytoconstituents responsible for its antibacterial activity through computational studies.

2 Materials and Methods

2.1 Plant material

The plant material was collected from local areas in the Kumaun region of Bhimtal, Uttarakhand, India, at an altitude of 1,370 meters. It was authenticated by Dr. K. Madhava Chetty, Associate Professor in the Department of Botany at Sri Venkateshwara University, Tirupati, Andhra Pradesh, India (Voucher specimen no. 1243). The plant material was dried in the shade at a temperature of approximately 40°C, then ground into a coarse powder and stored in an airtight container.

2.2 Extraction

The dried plant material was coarsely powdered and then subjected to continuous hot extraction with petroleum ether using a Soxhlet apparatus (Jones and Kinghorn 2012). After extraction, the resulting extract was concentrated using a rotary evaporator and then dried in a vacuum desiccator. The concentrated extract was transferred to a previously weighed china dish (Priscilla et al. 2024). Following the defatting process, the remaining marc was air-dried and subsequently extracted again using chloroform, ethyl acetate, and ethanol. The percentage yields of the different extracts were calculated, and the prepared extracts were stored in a desiccator for further use (Zhao et al. 2014).

2.3 Phytochemical screening

For chemical testing, various solvent extracts of *N. officinale* were evaluated, including petroleum ether extract (NOPE), chloroform extract (NOCE), ethyl acetate extract (NOEE), and alcoholic extract (NOAE). The screening was conducted using standard methods established by previous researchers (Farnsworth 1966; Dubale et al. 2023; Joshi et al. 2024).

2.4 Antimicrobial Activity Assay

2.4.1 Inoculum preparation

Nutrient agar slants were used to store bacterial stock cultures of *S. aureus*, which were obtained from IMTECH Chandigarh at 4°C. A sterile loop was used to transfer cells from the stock cultures into test tubes containing nutrient agar media to prepare active cultures for testing. The inoculated test tubes were then incubated at 37°C for 24 hours under static conditions, which means without agitation, to promote bacterial growth. After incubation, the bacterial cultures were diluted with nutrient broth to achieve a standardized optical density corresponding to approximately 2.0×10^6 colony-forming units (CFU) per milliliter. This standardization ensured uniformity for subsequent tests (Biemer 1971).

2.4.2 Test for Antimicrobial Susceptibility and Determination of Minimum Inhibitory Concentration (MIC)

Prepared extracts were tested against *S. aureus* (MTCC 96) to evaluate their antibacterial activity using the disc diffusion method. Each bacterium was cultivated in 20 ml of sterilized nutritional agar medium within sterilized Petri plates. Once the medium solidified, the inoculum suspension was uniformly applied to the entire agar surface through a swabbing technique, spreading horizontally and then vertically to ensure even distribution of the bacteria across the agar (Ilieva et al. 2024; Kulathunga and Rubin 2017). Next, 6 mm filter paper discs infused with either 1 or 10 mg/ml solutions of the dry extract were placed on the agar plates (Huang et al. 2024). After allowing the extracts to diffuse for five

minutes, the plates were incubated at 37°C for 24 hours. Additionally, antibiotic discs (Hexa-G) were used as positive controls. The inhibition zones were measured using a Hi-media zone measuring ruler, and all experiments were conducted in duplicate (Hemeg et al. 2020; Dubale et al. 2023). To determine the minimum inhibitory concentration (MIC), fresh cultures were prepared in 5 ml nutrient broth tubes. Different concentrations (3, 5, 10, 15, 20, and 25 µg/ml) of the potent extract were added to the tubes (Hemeg et al. 2020). A 0.1 ml sample of the freshly cultured bacteria was introduced into each tube. Negative controls comprised tubes without any treatment, while positive controls contained tubes inoculated with bacteria and clindamycin. After incubating the tubes at 37°C, the cultures were examined at 24 and 48 hours. The minimum concentration that resulted in the least bacterial growth was recorded as the MIC (Barnes et al. 2023).

2.5 Thin Layer Chromatographic Profile (TLC) for Standardization

Thin Layer Chromatography (TLC) is often used as a reference or cross-validation technique for more complex analytical methods such as High-Performance Liquid Chromatography (HPLC) or Gas Chromatography (GC). It acts as a simple confirmatory test in laboratories, helping to identify compounds by comparing their retention factor (Rf) to that of standards. In this experiment, TLC was performed using a mixture of toluene and ethyl acetate as the eluent in an 8:2 ratio. The Camag Linomat 5 automated TLC applicator was employed to apply the sample in 6 mm-wide bands at a nitrogen flow rate of 90 nL/s. After the sample was applied, the plate was allowed to dry before being placed in a chromatographic tank, which was promptly covered. Once the solvent front reached the top of the plate, it was removed, labeled, and left to dry. Finally, the plate was examined under UV light at wavelengths of 254 nm and 366 nm (Mayasari et al. 2022).

2.6 Molecular Docking Studies of *N. officinale* Phytoconstituents

2.6.1 Collection of Phytoconstituents of *N. officinale* and Preparation of Ligand Molecules

After conducting an extensive literature search, it was found that *N. officinale* contains a variety of phytoconstituents, including apigenin, beta-carotene, caffeic acid, carvacrol, eucalyptol, gallic acid, isorhamnetin, kaempferol, lutein, luteolin, pulegone, quercetin, and rutin. A molecular docking study related to drug-receptor interactions indicates that biological activity is directly linked to these interactions. The significance of molecular docking lies in its ability to identify the phytoconstituents with the highest likelihood of effectiveness against microbes, suggesting potential antimicrobial activity. All molecular structures were prepared using Avogadro software and

AutoDock Tools (version 1.5.6). The ligand molecules were saved in .PDBQT format (Hanwell et al. 2012).

2.6.2 Procurement and Preparation of Receptor

In this manuscript, we focused on a topoisomerase ATPase inhibitor, specifically targeting DNA gyrase. This enzyme is selective for bacterial species, and its inhibition disrupts DNA synthesis, ultimately leading to cell death. The receptor discussed, identified as 3TTZ, is from *S. aureus*. The receptor comprises two chains, each consisting of 198 amino acids. Within the receptor, the complexed ligand, 2-[(3S,4R)-4-[(3,4-dichloro-5-methyl-1H-pyrrol-2-yl)carbonyl]amino}-3-fluoropiperidin-1-yl]-1,3-thiazole-5-carboxylic acid (07N), was detected (Sherer et al. 2011). This complexed ligand interacts with amino acids ARG 144, PRO 87, ASN 54, ILE 86, ILE 51, ILE 175, VAL 79, ARG 84, and GLU 58 (Paggi et al. 2024). After removing the complex ligand and water molecules, we added polar hydrogens and Gasteiger charges (Bisht et al. 2024). Finally, the receptor was saved in .PDBQT format. The grid box dimensions for the 3TTZ receptor were 7.751, 5.062, and 20.947 along the x, y, and z axes, respectively (Goodsell et al. 2021).

2.7 Molecular Dynamic (MD) Simulation of Selected Phytoconstituents of *N. officinale*

Molecular docking of the phytoconstituents revealed that isorhamnetin achieved the highest molecular docking score. While molecular docking is performed in a vacuum, molecular dynamics (MD) simulation is carried out in a realistic simulated environment using the best-docked isorhamnetin. Through MD simulation, the atomic-level interaction patterns of isorhamnetin with the receptor were identified in the presence of solvent, ions, temperature, pressure, and a CHARMM force field environment. TIP3 water was used for the simulation, conducted with GROMACS version 20.1 software. Prior to the simulation, the ligand-receptor complex underwent energy minimization (Kim et al. 2017). During the preparation of isorhamnetin for the simulation study, 8,701 water molecules and 11 sodium ions were incorporated into the system. The graphical representation of the simulation trajectories was created using Qtgrace software (Lemkul 2018).

2.8 Statistical Analysis

The results were presented as Mean ± SEM (Standard Error Mean) with n=3. The data were analyzed using ANOVA in GraphPad Prism 6.

3 Results and Discussion

3.1 Phytochemical Screening and Extraction Yield

The percentage yields (% w/w) of the extracts NOPE, NOEE, NOCE, and NOAE from *N. officinale* were found to be 20.37%,

Table 1 Phytochemical analysis of different extracts of *N. officinale*

Phytochemical	Tests (Dubale et al. 2023)	NOPE	NOCE	NOEE	NOAE
Amino acids	Ninhydrin test	+	-	-	+
Proteins	Biuret test	+	-	-	+
	Millon's test	+	-	-	+
Carbohydrates	Molisch's test	-	-	-	+
	Fehling's test	-	-	-	+
Steroids	Salkowski Reaction	-	-	-	-
Alkaloids	Mayer's test	-	+	-	-
	Dragendroff's test	-	+	-	-
	Hager's test	-	+	-	-
Glycosides	Legal	-	-	-	+
	Keller kiliani Test	-	-	-	+
	Borntrager's test	-	-	-	-
	Foam test	-	-	-	+
Flavonoids	Shinoda's test	-	+	+	-
Phenolic compounds	FeCl ₃ test	-	+	+	+
	Lead acetate solution test	-	+	+	+

+ positive; - negative

20.90%, 21.72%, and 18.69%, respectively. These findings indicate that the plant extracts contain various compounds, including proteins, alkaloids, tannins, polyphenols, flavanones, and reducing sugars (Ercan and Dođru 2023) (Table 1). *N. officinale* is a semi-aquatic plant known for its diverse array of chemical compounds and numerous therapeutic activities. The percentage yield of these extracts depends on the specific parts of the plant used, the species, and the solvent employed for extraction. Different parts of the plant contain varying concentrations of secondary metabolites, which contribute to many of the plant's beneficial properties. This suggests that *N. officinale* may serve as a valuable source of medicinal compounds, highlighting its significance in therapeutic applications. Furthermore, several solvent extracts were analyzed for specific chemical components, such as alkaloids, glycosides, flavonoids, and tannins, through phytochemical analysis. The anticancer potential of the phytochemicals found in *N. officinale* has been documented in previous studies (Negi et al. 2024b).

3.2 Antimicrobial activity of *N. officinale*

The antimicrobial properties of different extracts of *N. officinale* against *S. aureus* were evaluated using a disk diffusion method. The zones of inhibition for each tested extract were measured and are shown in Figure 1. Among the extracts evaluated, the NOCE exhibited the highest zones of inhibition, measuring 14.0

mm at a concentration of 1 mg/ml and 24.0 mm at 10 mg/ml. The NOEE demonstrated the second-highest zones of inhibition, with 12.0 mm at 1 mg/ml and 16.0 mm at 10 mg/ml. These results are comparable to the inhibition zones of the standard antibiotic clindamycin, which showed 16.0 mm and 29.0 mm at the same respective concentrations. All *N. officinale* extracts displayed observable zones of inhibition against *S. aureus* (Figure 2). Notably, NOCE exhibited the best antimicrobial activity across various dilutions during 4 hours (Tittikpina et al. 2018; Necedo-Mena et al. 2020). Additionally, the minimum inhibitory concentration (MIC) of the most effective extract (NOCE) was determined using different concentrations (3, 5, 10, 15, 20, 25 µg/ml). The potent MIC observed was 3 µg/ml, as shown in Table 2 (Mabhiza et al. 2016; Nair et al. 2017; Farhadi et al. 2019). Since the MIC represents the lowest concentration at which inhibition occurs, only this concentration is reported. Though inhibition was observed at 3 µg/mL, it is evident that higher concentrations also contributed to significant zones of inhibition. The findings of this investigation are consistent with the work of Jang et al. (2010), which indicated that *N. officinale* has a greater inhibitory effect on gram-positive bacteria, such as *S. aureus*, compared to gram-negative bacteria. Supporting evidence can also be found in the studies by Butnariu and Bostan (2011) and Mahdavi et al. (2019), which suggested that the antimicrobial activity of *N. officinale* has a bacteriostatic effect on *S. aureus*.

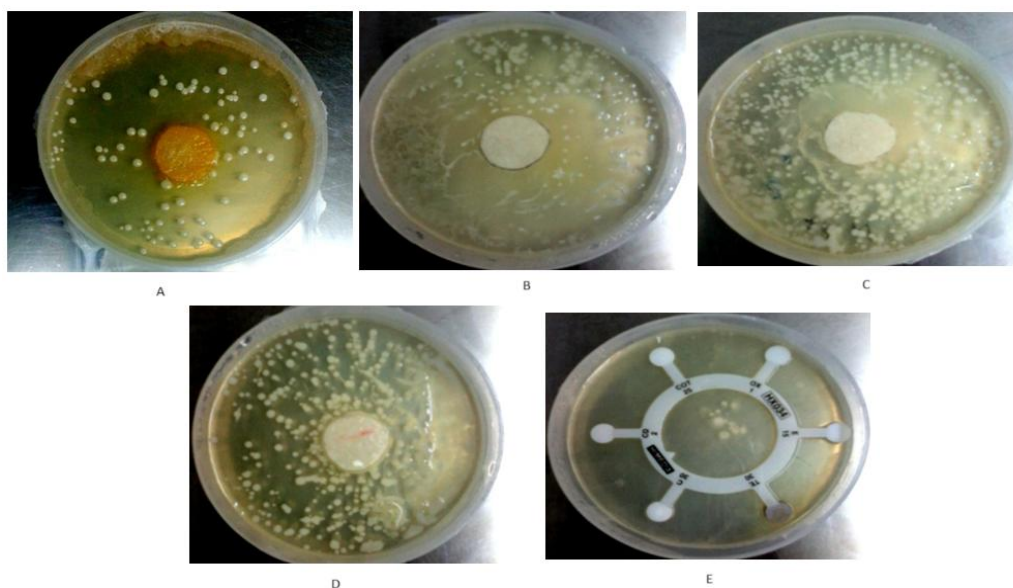


Figure 1 Antimicrobial activity of the different extracts of *N. officinale*; where A: NOCE, B: NOEE, C: NOAE, D: NOPE, E: HEXA G PLUS- 11 against *S. aureus*

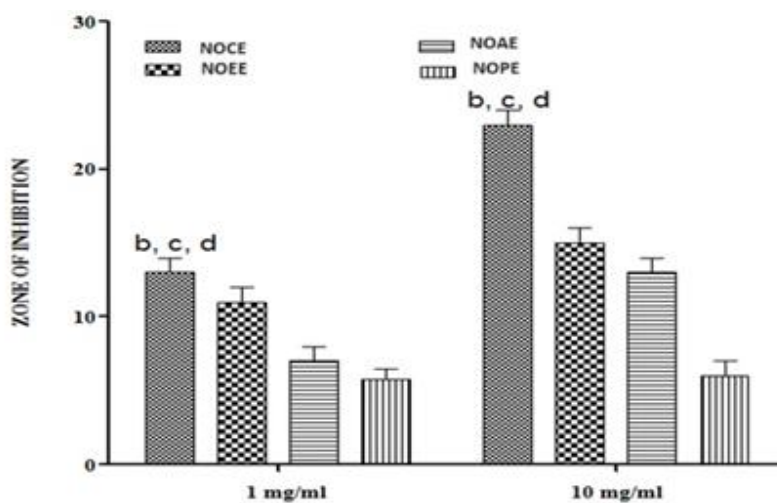


Figure 2 Bar diagram representing the antimicrobial activity of the different extracts of *N. officinale*. All the values expressed are Mean \pm SD (n=3), ^a P < 0.05 Vs NOCE; ^{b, c, d} P < 0.05 Vs NOEE, NOAE, NOPE.

Table 2 Result of zone of inhibition of potent antimicrobial extract (NOCE) at different concentrations

Extract	Concentration (μ g/ml)	Zone of inhibition (mm)
NOCE	3	26.0
	5	NA
	10	NA
	15	NA
	20	NA
	25	NA

NA: Not Applicable

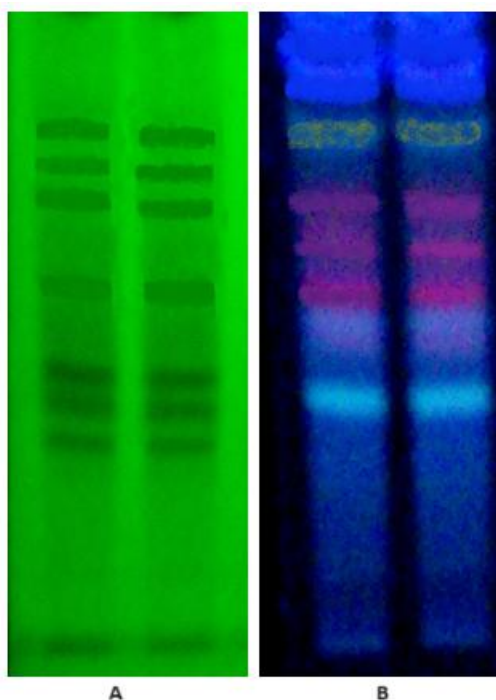


Figure 3 TLC fingerprinting profile of NOCE extract, where (A) under short and (B) long UV, respectively.

Table 3 Detail of the TLC profile of active extract (NOCE) under short UV (254 nm) and long UV (366 nm)

Extract	Rf in long UV (366 nm)	Rf in short UV (254 nm)
NOCE	0.20, 0.25, 0.31, 0.38, 0.44, 0.51, 0.61, 0.69, 0.73, 0.81	0.21, 0.28, 0.35, 0.40, 0.46, 0.51, 0.65, 0.82, 0.89

3.3 TLC fingerprinting profiles of NOCE

In the TLC (Thin Layer Chromatography) fingerprint profile, NOCE exhibited 10 spots in the long UV range and 9 spots in the short UV range, as shown in Figure 3 and Table 3. This study confirmed that NOCE contains a variety of phytoconstituents, indicated by the multiple spots observed at different RF (retention factor) values. Among the tested classes of compounds, the phytochemicals exhibiting the most significant color changes were flavonoids, alkaloids, and phenols (Ayele et al. 2015). The resulting chromatogram can serve as additional information for the identification and standardization of *N. officinale*.

3.4 Molecular Docking Analysis Data

The molecular docking study is focused on understanding drug-receptor interactions in a vacuum, which is directly related to the biological activity of drugs. The significance of this study lies in identifying which phytoconstituent has the highest probability of targeting microbes and contributing to antimicrobial activity. The molecular docking scores of the phytoconstituents from *N. officinale* against bacterial DNA gyrase ranged from -5.0 kcal/mol to -8.5 kcal/mol (Table 4). The top three phytoconstituents with the

highest docking scores were isorhamnetin (-8.5 kcal/mol), luteolin (-8.1 kcal/mol), and quercetin (-7.8 kcal/mol) (Kar et al. 2024). Isorhamnetin interacted with the receptor through several amino acids: ASN 54 (3.60 Å between interaction carbon atoms), ILE 86 (3.28 Å), and THR 173 (3.98 Å) via hydrophobic interactions. Additionally, it formed hydrogen bonds with ASN 54, GLU 58, ARG 84, GLY 85, and THR 173 (Yu et al. 2024). Luteolin interacted with the receptor through ILE 51 (3.68 Å), ILE 86 (3.58 Å), ILE 102 (3.33 Å), and LEU 103 (3.65 Å) via hydrophobic interactions. Its hydrogen bonds were formed with ASN 54, ARG 84, and GLY 85 (Rigby 2024). Quercetin interacted with the DNA gyrase receptor through ILE 51 (3.92 Å), ILE 86 (3.93 Å), THR 173 (3.74 Å), and ILE 175 (3.63 Å) via hydrophobic interactions. It also formed hydrogen bonds with GLU 58, ASP 81, and ARG 84 (Figure 4). The common amino acid residues shared between isorhamnetin and the complexed ligand include ASN 54, ILE 86, GLU 58, and ARG 84 (Lokhande et al. 2022). Luteolin and the complexed ligand share ILE 51, ILE 86, ASN 54, and ARG 84. Similarly, quercetin and the complexed ligand share ILE 51, ILE 86, GLU 58, and ARG 84. The docking scores and the active site residues suggest that isorhamnetin, luteolin, and quercetin interact effectively with the bacterial gyrase receptor, potentially contributing to their antibacterial activity (Notarte et al. 2023).

Table 4 Molecular docking interaction data of selected phytoconstituents of *N. officinale* against bacterial DNA gyrase

S. N.	Name	Dock score (kcal/mol)	Hydrophobic Interactions	Hydrogen bond Interactions
1.	Apigenin	-7.7	ASN 54 (distance between interaction carbon atoms 3.57 Å), ILE 86 (distance between interaction carbon atoms 3.31 Å), THR 173 (distance between interaction carbon atoms 3.84 Å).	ASN 54 (distance H-A 2.93 Å, D-A 3.64 Å), ARG84 (distance H-A 3.11 Å, D-A 3.67 Å), GLY 85 (distance H-A 2.66 Å, D-A 3.27Å), THR 173 (distance H-A 3.53 Å, D-A 3.87Å).
2.	Beta carotene	-6.9	GLU 68 (distance between interaction carbon atoms 3.54 Å), LYS 78 (distance between interaction carbon atoms 3.85 Å), THR 80 (distance between interaction carbon atoms 3.56 Å), TYR 141 (distance between interaction carbon atoms 3.76 Å), VAL 165 (distance between interaction carbon atoms 3.52 Å), VAL 174 (distance between interaction carbon atoms 3.58 Å).	None
3.	Caffeic acid	-6.7	ASN 54 (distance between interaction carbon atoms 3.45 Å), ILE 86 (distance between interaction carbon atoms 3.48 Å), THR 173 (distance between interaction carbon atoms 3.66 Å).	ASN 54 (distance H-A 3.58 Å, D-A 4.07Å), SER 55 (distance H-A 3.31 Å, D-A 3.74Å), GLU 58 (distance H-A 2.65 Å, D-A 2.94Å), ARG 84 (distance H-A 3.36 Å, D-A 3.90Å), GLY 85 (distance H-A 1.90 Å, D-A 2.83Å).
4.	Carvacrol	-5.9	ILE 51 (distance between interaction carbon atoms 3.60 Å), ASN 54 (distance between interaction carbon atoms 3.51 Å), ILE 86 (distance between interaction carbon atoms 3.66 Å), ILE 175 (distance between interaction carbon atoms 3.77 Å).	THR 173 (distance H-A 3.27Å, D-A 3.81Å).
5.	Eucalyptol	-5.0	ASN 54 (distance between interaction carbon atoms 3.66 Å), GLU 58 (distance between interaction carbon atoms 3.68 Å), ILE 102 (distance between interaction carbon atoms 3.77 Å).	None
6.	Gallic acid	-6.0	ARG 84 (salt bridge distance 4.19 Å).	ASN 54 (distance H-A 2.38 Å, D-A 3.23 Å), ASP 81 (distance H-A 2.17Å, D-A 3.06Å), GLY 85 (distance H-A 3.03 Å, D-A 3.87Å), ARG 144 (distance H-A 3.48 Å, D-A 4.08 Å).
7.	Isorhamnetin	-8.5	ASN 54 (distance between interaction carbon atoms 3.60 Å), ILE 86 (distance between interaction carbon atoms 3.28 Å), THR 173 (distance between interaction carbon atoms 3.98 Å).	ASN 54 (distance H-A 2.89 Å, D-A 3.63Å), GLU 58 (distance H-A 2.29Å, D-A 2.79Å), ARG 84 (distance H-A 3.18Å, D-A 3.74Å), GLY 85 (distance H-A 2.18Å, D-A 2.92Å), THR 173 (distance H-A 2.28 Å, D-A 2.79Å).
8.	Kaemferol	-7.5	ILE 51 (distance between interaction carbon atoms 3.74 Å), ILE 86 (distance between interaction carbon atoms 3.78 Å), THR 173 (distance between interaction carbon atoms 3.73 Å), ILE 175 (distance between interaction carbon atoms 3.48 Å).	None
9.	Lutein	-5.0	GLN 66 (distance between interaction carbon atoms 3.83 Å), GLU 68 (distance between interaction carbon atoms 3.64 Å), THR 80 (distance between interaction carbon atoms 3.64 Å), ILE 148 (distance between interaction carbon atoms 2.99 Å), LYS 163 (distance between interaction carbon atoms 3.68 Å), VAL 165 (distance between interaction carbon atoms 3.52 Å), VAL 174 (distance between interaction carbon atoms 3.36 Å).	GLN (distance H-A 1.74 Å, D-A 2.71Å), LYS 163 (distance H-A 3.32 Å, D-A 3.71Å), GLN 210 (distance H-A 3.18 Å, D-A 4.08Å).
10.	Luteolin	-8.1	ILE 51 (distance between interaction carbon atoms 3.68 Å), ILE 86 (distance between interaction carbon atoms 3.58 Å), ILE 102 (distance between interaction carbon atoms 3.33 Å), LEU 103 (distance between interaction carbon atoms 3.65 Å).	ASN 54 (distance H-A 3.41 Å, D-A 4.08Å), ARG 84 (distance H-A 2.90 Å, D-A 3.30Å), GLY 85 (distance H-A 2.33 Å, D-A 2.81Å).

S. N.	Name	Dock score (kcal/mol)	Hydrophobic Interactions	Hydrogen bond Interactions
11	Pulegone	-5.6	ASN 54 (distance between interaction carbon atoms 3.34 Å), ILE 86 (distance between interaction carbon atoms 3.58 Å), THR 173 (distance between interaction carbon atoms 3.76 Å), ILE 175 (distance between interaction carbon atoms 3.88 Å).	THR 173 (distance H-A 2.39 Å, D-A 3.15Å).
12	Quercetin	-7.8	ILE 51 (distance between interaction carbon atoms 3.92 Å), ILE 86 (distance between interaction carbon atoms 3.93 Å), THR 173 (distance between interaction carbon atoms 3.74 Å), ILE 175 (distance between interaction carbon atoms 3.63 Å).	GLU 58 (distance H-A 2.35 Å, D-A 2.95Å), ASP 81 (distance H-A 2.15 Å, D-A 3.00Å), ARG 84 (distance H-A 2.75 Å, D-A 3.27Å).
13	Rutin	-7.5	GLN 66 (distance between interaction carbon atoms 3.35 Å), THR 80 (distance between interaction carbon atoms 3.22 Å), TYR 141 (distance between interaction carbon atoms 3.72 Å), VAL 174 (distance between interaction carbon atoms 3.69 Å), LYS 170 (distance between interaction carbon atoms 3.51 Å).	ILE 67 (distance H-A 2.36 Å, D-A 2.84 Å), GLU 68 (distance H-A 2.56 Å, D-A 2.94 Å), HIS 143 (distance H-A 2.23 Å, D-A 3.06Å), LYS 170 (distance H-A 2.48 Å, D-A 2.90Å), GLN 210 (distance H-A 2.39Å, D-A 3.37Å), THR 212 (distance H-A 3.16 Å, D-A 3.81Å).

H-A= Distance between hydrogen and acceptor atom (Å); D-A= Distance between donor and acceptor atom (Å)

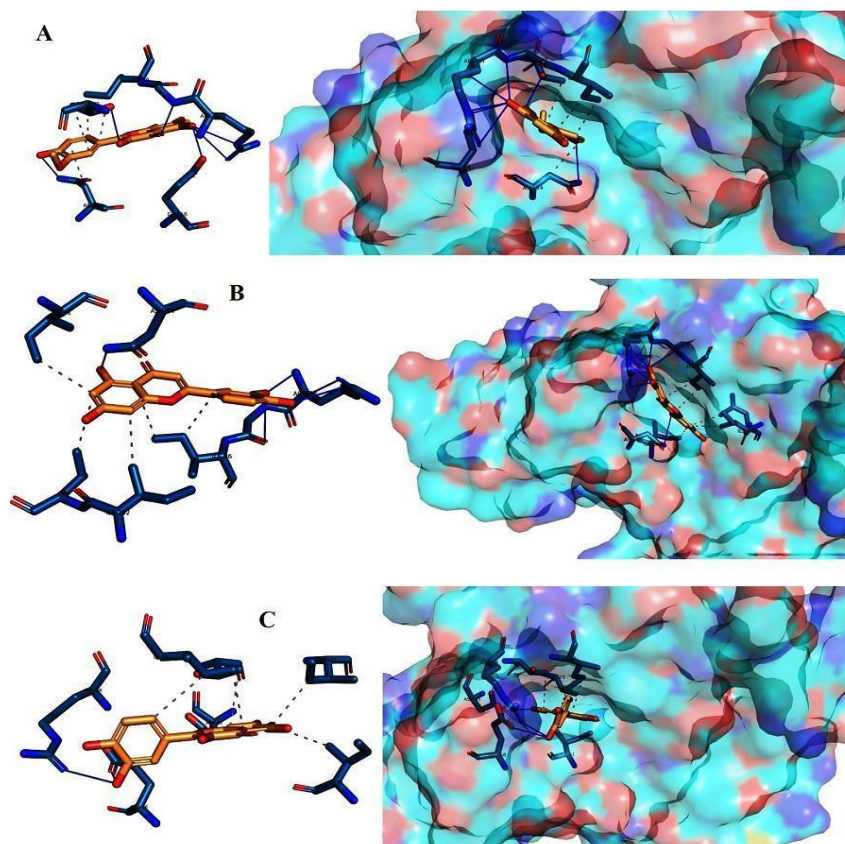


Figure 4 Molecular docking interactions data of Isorhamnetin (A), Luteolin (B), and Quercetin (C) against DNA gyrase

3.5 MD Simulation Analysis Data of Isorhamnetin with DNA gyrase

Molecular docking studies of the phytoconstituents indicated that isorhamnetin has the highest probability of interacting with bacterial gyrase, suggesting that the antibacterial activity of NOCE

may be attributed to isorhamnetin. Previous research has established the antibacterial effectiveness of isorhamnetin against *S. aureus* (Jiang et al. 2016; Suarez et al. 2021). As previously mentioned, molecular docking is conducted in a vacuum, whereas molecular dynamics (MD) simulations are performed in a realistically simulated environment using the best-docked structure

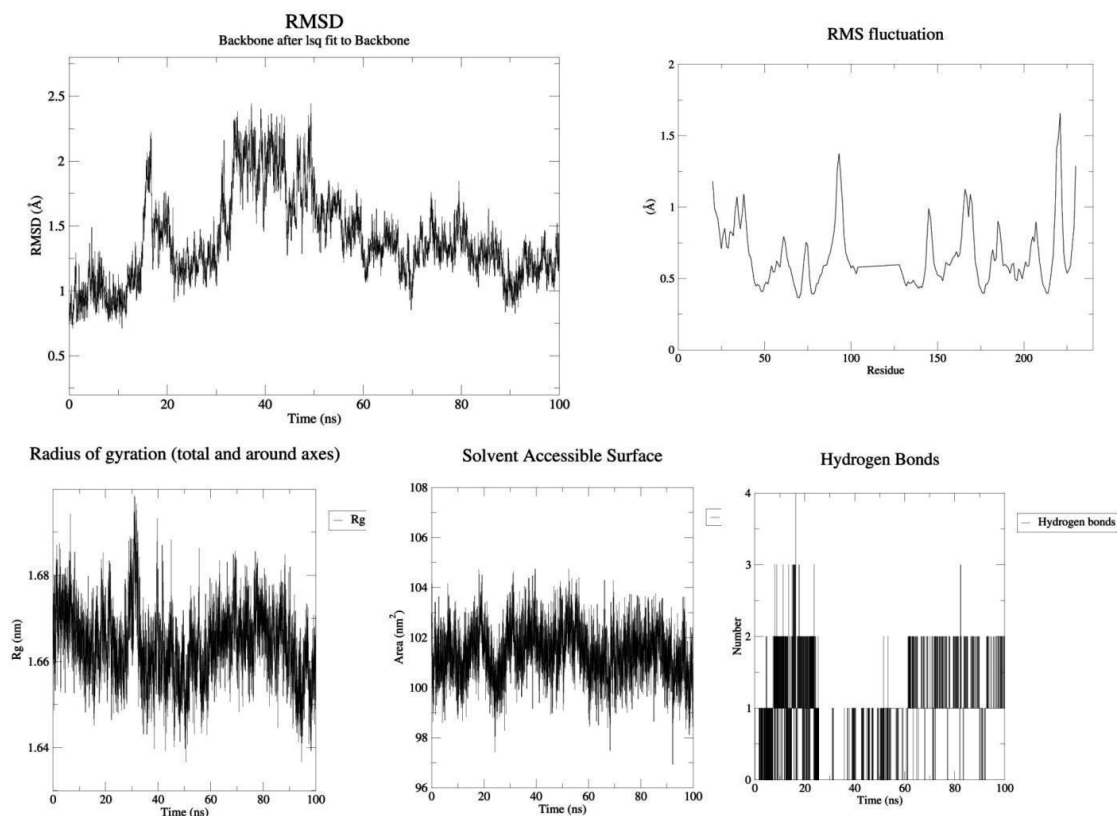


Figure 5 MD Simulation data of isorhamnetin interacted with DNA gyrase.

of isorhamnetin (Khan et al. 2024). Through MD simulations, we were able to identify atomic-level interaction patterns of isorhamnetin within the receptor in the presence of solvent, ions, temperature, pressure, and a CHARMM force field environment. The average root mean square deviation (RMSD) value for isorhamnetin was found to be 1.38 Å. The RMSD stabilized at 60 ns of simulation time, and during the simulation, both molecules maintained a similar interaction pattern (Dos Santos Nascimento and de Moura 2024). The root mean square fluctuation (RMSF) diagram indicated that fluctuations were generally limited to 1.6 Å during most of the simulation runs (Prinsa et al. 2024). Notably, isorhamnetin displayed considerable fluctuations near the 221st amino acid residue within the receptor and exhibited maximum fluctuations during the simulation, likely because these residues were either absent during interactions or located at a distance from the active site (Kushwaha et al. 2021). The average radius of gyration for the isorhamnetin complex with the receptor was measured at 1.66 nm, demonstrating a constant value without any significant fluctuation. The radius of gyration values remained within a lower range, indicating that the molecules were consistently contained within the receptor's active site throughout the simulation (Jalali et al. 2024). Additionally, the average solvent-accessible surface area (SASA) of the isorhamnetin complex with the bacterial DNA gyrase receptor was 101.38 nm²

(Zhong et al. 2024). The SASA values confirmed the formation of stable structures during the simulation (Kumari and Kumar 2014). The hydrogen bond interaction map confirmed that isorhamnetin remained complexed with the bacterial DNA gyrase receptor throughout the simulation, and the ligand molecule maintained contact with the active site amino acid residues, indicating a strong relationship between the ligand and receptor (Figure 5) (Kawsar et al. 2024).

Conclusion

In this manuscript, we demonstrate that the chloroform extract of *N. officinale* exhibits the most potent antibacterial activity. Molecular docking studies of the phytoconstituents of *N. officinale* against bacterial DNA gyrase indicated that isorhamnetin achieved the highest docking score. Molecular dynamics (MD) simulations of isorhamnetin interacting with bacterial DNA gyrase showed that all parameters remained within acceptable limits. These findings confirm that *N. officinale* has significant antibacterial properties, likely attributed to isorhamnetin.

Abbreviations

Nasturtium officinale petroleum ether extract (NOPE), *Nasturtium officinale* chloroform extract (NOCE), *Nasturtium officinale* ethyl

acetate extract (NOEE), and *Nasturtium officinale* alcoholic extract (NOAE)

Conflict of Interest

Nil

Ethical Clearance

No animal model was used in the study; therefore, ethical clearance is not required.

References

Akbari Bazm, M., Khazaei, M., Khazaei, F., & Naseri, L. (2019). *Nasturtium Officinale* L. hydroalcoholic extract improved oxymetholone-induced oxidative injury in mouse testis and sperm parameters. *Andrologia*, 51(7), e13294.

Ayele, T. T., Regasa, M. B., & Delesa, D. A. (2015). Antibacterial and antagonistic activity of selected traditional medicinal plants and herbs from East Wollega Zone against clinical isolated human pathogens. *Science, Technology and Arts Research Journal*, 4(3), 175-179.

Barnes, V.L., Heithoff, D.M., Mahan, S.P., House, J.K., & Mahan, M.J. (2023). Antimicrobial susceptibility testing to evaluate minimum inhibitory concentration values of clinically relevant antibiotics. *STAR Protocols*, 4(3), 102512.

Biemer, J.J. (1971). Antimicrobial susceptibility testing by the Kirby-Bauer disc diffusion method. *Annals of Clinical & Laboratory Science*, 3(2), 135-40.

Bisht, A., Tewari, D., Kumar, S., & Chandra, S. (2024). Network pharmacology, molecular docking, and molecular dynamics simulation to elucidate the mechanism of anti-aging action of *Tinospora cordifolia*. *Molecular Diversity*, 28(3), 1743-1763.

Butnariu, M., & Bostan, C. (2011). Antimicrobial and anti-inflammatory activities of the volatile oil compounds from *Tropaeolum majus* L.(Nasturtium). *African journal of biotechnology*, 10(31), 5900-5909.

Dos Santos Nascimento, I.J., & de Moura, R.O. (2024). Molecular Dynamics Simulations in Drug Discovery. *Mini Reviews in Medicinal Chemistry*, 24(11), 1061-1062.

Dubale, S., Kebebe, D., Zeynudin, A., Abdissa, N., & Suleman, S. (2023). Phytochemical screening and antimicrobial activity evaluation of selected medicinal plants in Ethiopia. *Journal of experimental pharmacology*, 15, 51-62.

Ercan, L., & Dođru, M. (2023). Determination of phenolic compounds in *Nasturtium Officinale* by LC-MS/MS using

different extraction methods and different solvents. *International Journal of Chemistry and Technology*, 7(2), 124-130.

Farhadi, F., Khameneh, B., Iranshahi, M., & Iranshahi, M. (2019). Antibacterial activity of flavonoids and their structure–activity relationship: An update review. *Phytotherapy Research*, 33(1), 13-40.

Farnsworth, N. R. (1966). Biological and phytochemical screening of plants. *Journal of Pharmaceutical Sciences*, 55(3), 225-276.

Goodsell D.S., Sanner M.F., Olson A.J., & Forli S. (2021). The AutoDock suite at 30. *Protein Science*, 30(1) 31-43.

Hanwell M.D., Curtis D.E., Lonie, D.C., Vandermeersch T., Zurek E., & Hutchison G.R. (2012). Avogadro: an advanced semantic chemical editor, visualization, and analysis platform. *Journal of Cheminformatics*, 4, 17.

Hemeg, H.A., Moussa, I.M., Ibrahim, S., Dawoud, T.M., Alhaji, J.H., et al. (2020). Antimicrobial effect of different herbal plant extracts against different microbial population. *Saudi Journal of Biological Sciences*, 27(12), 3221-3227.

Hibbert, L.E., Qian, Y., Smith, H.K., Milner, S., Katz, E., Kliebenstein, D.J., & Taylor, G. (2023). Making watercress (*Nasturtium officinale*) cropping sustainable: genomic insights into enhanced phosphorus use efficiency in an aquatic crop. *Frontiers in Plant Science*, 14, 1279823.

Huang, H., Zhang, Y., Du, Q., Zheng, C., Jin, C., & Li, S. (2024). Synthesis and Antimicrobial Activity of 3-Alkylidene-2-Indolone Derivatives. *Molecules*, 29(22), 5384.

Ilieva, Y., Zaharieva, M.M., Najdenski, H., & Kroumov, A.D. (2024). Antimicrobial Activity of *Arthrospira* (Former *Spirulina*) and *Dunaliella* Related to Recognized Antimicrobial Bioactive Compounds. *International Journal of Molecular Sciences*, 25(10), 5548.

Jalali, P., Nowroozi, A., Moradi, S., & Shahlaei, M. (2024). Exploration of lipid bilayer mechanical properties using molecular dynamics simulation. *Archives of Biochemistry and Biophysics*, 761, 110151.

Jang, M., Hong, E., & Kim, G. H. (2010). Evaluation of antibacterial activity of 3-butenyl, 4-pentenyl, 2-phenylethyl, and benzyl isothiocyanate in *Brassica vegetables*. *Journal of food science*, 75(7), M412-M416.

Jiang, L., Li, H., Wang, L., Song, Z., Shi, L., Li, W., Deng, X., & Wang, J. (2016). Isorhamnetin Attenuates *Staphylococcus aureus* Induced Lung Cell Injury by Inhibiting Alpha-Hemolysin Expression. *Journal of Microbiology and Biotechnology*, 26(3), 596-602.

- Jones, W.P., & Kinghorn, A.D. (2012). Extraction of plant secondary metabolites. *Methods in Molecular Biology*, 864, 341-66.
- Joshi, B.C., Juyal, V., & Sah, A.N. (2024). First Report on Pharmacognostic, Phytochemical Investigation and In vitro Radical Scavenging Efficacy of *Premna barbata* from Western Himalaya. *Proceedings of the National Academy of Sciences, India Section B: Biological Sciences*, 94, 685–695.
- Kar, P., Oriola, A.O., & Oyediji, A.O. (2024). Molecular Docking Approach for Biological Interaction of Green Synthesized Nanoparticles. *Molecules*, 29(11), 2428.
- Kawsar, S.M.A., Hossain, M.A., Saha, S., Abdallah, E.M., Bhat, A.R., Ahmed, S., Jamalis, J., & Ozeki Y. (2024). Nucleoside-Based Drug Target with General Antimicrobial Screening and Specific Computational Studies against SARS-CoV-2 Main Protease. *Chemistry Select*, 9, e202304774.
- Khan, M.I., Pathania, S., Al-Rabia, M.W., Ethayathulla, A.S., Khan, M.I., et al. (2024). MolDy: molecular dynamics simulation made easy. *Bioinformatics*, 40(6), btae313.
- Kim S., Lee J., Jo S., Brooks C.L. 3rd., Lee H.S., & Im W. (2017). CHARMM-GUI ligand reader and modeler for CHARMM force field generation of small molecules. *Journal of Computational Chemistry*, 38(21) 1879-1886.
- Klimek-Szczykutowicz, M., Szopa, A., & Ekiert, H. (2018). Chemical composition, traditional and professional use in medicine, application in environmental protection, position in food and cosmetics industries, and biotechnological studies of *Nasturtium officinale* (watercress) - a review. *Fitoterapia*, 129, 283-292.
- Kulathunga, D.G., & Rubin, J.E. (2017). A review of the current state of antimicrobial susceptibility test methods for Brachyspira. *Canadian Journal of Microbiology*, 63(6), 465-474.
- Kumari, R., & Kumar, R. (2014). Open Source Drug Discovery Consortium, Lynn A. g_mmpbsa-A GROMACS Tool for High-Throughput MM-PBSA Calculations. *Journal of Chemical Information and Modeling*, 54(7), 1951–1962.
- Kushwaha, P.P., Singh, A.K., Bansal, T., Yadav, A., Prajapati, K.S., Mohd, S., & Kumar, S. (2021). Identification of Natural Inhibitors Against SARSCoV-2 Drugable Targets Using Molecular Docking, Molecular Dynamics Simulation, and MM-PBSA Approach. *Frontier Cellular Infection Microbiology*, 11, 730288.
- Lemkul, J.A. (2018). From Proteins to Perturbed Hamiltonians: A Suite of Tutorials for the GROMACS-2018 Molecular Simulation Package, v1.0^o. *Living Journal of Computational Molecular Science*, 1(1), 5068.
- Lokhande, K., Nawani, N.K., Venkateswara, S., & Pawar, S. (2022). Biflavonoids from *Rhus succedanea* as probable natural inhibitors against SARS-CoV-2: a molecular docking and molecular dynamics approach. *Journal of Biomolecular Structure Dynamics*, 40(10), 4376-4388.
- Mabhiza, D., Chitemerere, T., & Mukanganyama, S. (2016). Antibacterial properties of alkaloid extracts from *Callistemon citrinus* and *Vernonia adoensis* against *Staphylococcus aureus* and *Pseudomonas aeruginosa*. *International Journal of Medicinal Chemistry*, 2016(1), 6304163.
- Mahdavi, S., Kheyrollahi, M., Sheikhlouei, H., & Isazadeh, A. (2019). Antibacterial and antioxidant activities of essential oil on food borne bacteria. *The Open Microbiology Journal*, 13(1), 81-85.
- Mayasari, D., Murti, Y.B., Pratiwi, S.U.T., Sudarsono, S., Hanna, G., & Hamann, M.T. (2022). TLC-Based Fingerprinting Analysis of the Geographical Variation of *Melastoma malabathricum* in Inland and Archipelago Regions: A Rapid and Easy-to-Use Tool for Field Metabolomics Studies. *Journal of Natural Products*, 85(1), 292-300.
- Mostafazadeh, M., Sadeghi, H., Sadeghi, H., Zarezade, V., Hadinia, A., & Panahi Kokhdan, E. (2022). Further evidence to support acute and chronic anti-inflammatory effects of *Nasturtium officinale*. *Research in Pharmaceutical Sciences*, 17(3), 305-314.
- Nair, J.J., Wilhelm, A., Bonnet, S.L., & van Staden, J. (2017). Antibacterial constituents of the plant family Amaryllidaceae. *Bioorganic & Medicinal Chemistry Letters*, 27(22), 4943-4951.
- Negi, N., Upadhyay, S., & Rana, M. (2024a). An Overview on Phytopharmacological Perspectives of a Potential plant Species: *Nasturtium officinale*. *Systematic Reviews in Pharmacy*, 15(8), 257-262.
- Negi, N., Upadhyay, S., & Rana, M. (2024b). Investigation of in vitro anticancer potential and phytochemical screening of *Nasturtium officinale*. *International Journal of Zoological Investigations*, 10(1), 537-544.
- Nocedo-Mena, D., Garza-González, E., González-Ferrara, M., & Del Rayo Camacho-Corona, M. (2020). Antibacterial Activity of *Cissus incisa* Extracts against Multidrug- Resistant Bacteria. *Current Topics in Medicinal Chemistry*, 20(4), 318-323.
- Notarte, K.I.R., Quimque, M.T.J., Macaranas, I.T., Khan, A., Pastrana, A.M., et al. (2023). Attenuation of Lipopolysaccharide-induced Inflammatory Responses through Inhibition of the NF-κB

- Pathway and the Increased NRF2 Level by a Flavonol-enriched n-Butanol Fraction from *Uvaria alba*. *ACS Omega*, 8(6), 5377–5392.
- Paggi, J.M., Pandit, A., & Dror, R.O. (2024). The Art and Science of Molecular Docking. *Annual Review of Biochemistry*, 93(1), 389-410.
- Prinsa., Saha, S., Bulbul, M.Z.H., Ozeki, Y., Alamri, M.A., & Kawsar, S.M.A. (2024). Flavonoids as potential KRAS inhibitors: DFT, molecular docking, molecular dynamics simulation and ADMET analyses. *Journal of Asian Natural Product Research*, 26(8), 955-992.
- Priscilla, K., Sharma, V., Gautam, A., Gupta, P., Dagar, R., Kishore, V., & Kumar, R. (2024). Carotenoid Extraction from Plant Tissues. *Methods in Molecular Biology*, 2788, 3-18.
- Rigby, S.P. (2024). Uses of Molecular Docking Simulations in Elucidating Synergistic, Additive, and/or Multi-Target (SAM) Effects of Herbal Medicines. *Molecules*, 29(22), 5406.
- Shakerinasab, N., Mottaghpisheh, J., Eftekhari, M., Sadeghi, H., Bazarganipour, F., Abbasi, R., Doustimotlagh, A.H. & Iriti, M. (2024). The hydroalcoholic extract of *Nasturtium officinale* reduces oxidative stress markers and increases total antioxidant capacity in patients with asthma. *Journal of Ethnopharmacology*, 318, 116862.
- Sherer, B.A., Hull, K., Green, O., Basarab, G., Hauck, S., et al. (2011). Pyrrolamide DNA gyrase inhibitors: Optimization of antibacterial activity and efficacy. *Bioorganic & medicinal chemistry letters*, 21(24), 7416-7420.
- Suarez, A.F.L., Tirador, A.D.G., Villorente, Z.M., Bagarinao, C.F., Sollesta, J.V.N., et al. (2021). The Isorhamnetin-Containing Fraction of Philippine Honey Produced by the Stingless Bee *Tetragonula biroi* Is an Antibiotic against Multidrug-Resistant *Staphylococcus aureus*. *Molecules*, 26(6), 1688.
- Tabesh, M., Sh, M.E., Etemadi, M., Naddaf, F., Heidari, F., & Alizargar, J. (2022). The antibacterial activity of *Nasturtium officinale* extract on common oral pathogenic bacteria. *Nigerian Journal of Clinical Practice*, 25(9), 1466-1475.
- Tittikpina, N.K., Nana, F., Fontanay, S., Philippot, S., Batawila, K., et al. (2018). Antibacterial activity and cytotoxicity of *Pterocarpus erinaceus* Poir extracts, fractions and isolated compounds. *Journal of Ethnopharmacology*, 212, 200-207.
- Yu, D., Li, H., Liu, Y., Yang, X., Yang, W., Fu, Y., Zuo, Y.A., & Huang, X. (2024). Application of the molecular dynamics simulation GROMACS in food science. *Food Research International*, 190, 114653.
- Zhao, S., Baik, O.D., Choi, Y.J., & Kim, S.M. (2014). Pretreatments for the efficient extraction of bioactive compounds from plant-based biomaterials. *Critical Reviews in Food Science and Nutrition*, 54(10), 1283-97.
- Zhong, H., Liu, H., & Liu, H. (2024). Molecular Mechanism of Tau Misfolding and Aggregation: Insights from Molecular Dynamics Simulation. *Current Medicinal Chemistry*, 31(20), 2855-2871.